International Journal of Pharmaceutics 373 (2009) 116–123

Contents lists available at ScienceDirect

International Journal of Pharmaceutics

journal homepage: www.elsevier.com/locate/ijpharm

Pharmaceutical Nanotechnology

Targeted delivery of doxorubicin using stealth liposomes modified with transferrin

XueMing Li[a,b], LiYan Ding[b], Yuanlong Xu[b], Yonglu Wang[b], QiNeng Ping[a,*]

[a] Department of Pharmaceutics, China Pharmaceutical University, Nanjing, China
[b] College of Life Science and Pharmaceutics, Nanjing University of Technology, Nanjing, China

ARTICLE INFO

Article history:
Received 11 June 2008
Received in revised form 23 January 2009
Accepted 25 January 2009
Available online 4 February 2009

Keywords:
Transferrin
Stealth liposomes
Intracellular delivery
Antitumor efficiency
Biodistribution
Targeting

ABSTRACT

Site-specific delivery of drugs and therapeutics can significantly reduce drug toxicity and increase the therapeutic effect. Transferrin (Tf) is one suitable ligand to be conjugated to drug delivery systems to achieve site-specific targeting, due to its specific binding to transferrin receptors (TfR), highly expressed on the surfaces of tumor cells. Stealth liposomes are effective vehicles for drugs, genes and vaccines and can be easily modified with proteins, antibodies, and other appropriate ligands, resulting in attractive formulations for targeted drug delivery. In this study, we prepared doxorubicin-loaded stealth liposomes (Tf-SL-DOX) by film dispersion followed by ammonium sulphate gradient method, then conjugated Tf to the liposome surface by an amide bound between DSPE–PEG_{2000}–COOH and Tf. The results of the intracellular uptake study indicated that Tf-modified SL was able to enhance the intracellular uptake of the entrapped DOX by HepG2 cells compared to SL-DOX. We studied tissue distribution and therapeutic effects of Free DOX, SL-DOX and Tf-SL-DOX in tumor-bearing mice and pharmacokinetics in rats. The pharmacokinetic behavior of Tf-SL-DOX in the plasma was closed to SL-DOX. Administration of Tf-SL-DOX to tumor-bearing mice could be used to deliver DOX effectively to the targeted site, significantly increasing DOX concentration in tumor and decreasing DOX concentration in heart and kidney. In summary, our study indicated that the Tf-coupled PEG liposomes (Tf-SL) could be as the targeted carriers to facilitate the delivery of the encapsulated anticancer drugs into tumor cells by receptor-mediated way.

1. Introduction

In the last two decades, many studies focused on developing drug delivery systems to achieve controlled release or enable drug targeting to specific tumor sites. Stealth liposomes (SL) have shed light on their use as potent drug carriers, since these have the ability to escape from the reticuloendothelial system (RES) and circulate in the blood for a long period (Ceh et al., 1997). It has been demonstrated that SL can accumulate in tumor tissue due to the effect of enhanced permeability and retention (EPR) (Maeda et al., 2000; Harrington et al., 2001).

However, anticancer drugs accumulation in tumor tissue via SL seems to be prerequisite but far from sufficient to guarantee a therapeutic improvement. For a variety of chemotherapeutic agents with an intracellular site of action, efficient intracellular uptake by the tumor cells should be the determinant step for their antitumor activity. While introducing PEG enables liposomes accumulate in tumor tissue, it creates a steric barrier that could cause a reduction in liposomes interaction with the target cells (Harvie et al., 2000; Vertut-Doi et al., 1996), leading to low uptake of the entrapped drugs via cell endocytosis or membrane fusion. In addition, various ligands or antibodies can be further attached to the surface-granted PEG chains, thus permitting them to be actively taken up by the target cells via receptor-mediated endocytosis.

The high specificity of endocytic uptake of transferrin (Tf) by the transferrin receptor (TfR) has made it a subject of interest for targeted drug delivery (Qian et al., 2002). The TfR is expressed in many tissue types in the body, particularly, in areas that feature a high turnover rate of cells. Elevated expression levels of TfR in neoplastic carcinomas show a good correlation between the number of TfR expressed and the proliferative ability of the tumor (Joo and Kim, 2002). The knowledge of TfR-over-expression in tumor tissues had led to a focused targeting of TfR in anticancer therapy (Anabousi et al., 2006), and subsequently to a number of small drugs and colloidal carrier systems linked to Tf (Singh et al., 1998).

Ishida et al. (2001) demonstrated the utility of Tf-coupled PEG liposomes (Tf-SL) for the intracellular targeting of the liposomes to tumor cells via receptor-mediated endocytosis. They also indicated that small liposomes with a diameter of 60 nm were taken up by tumor cells by receptor-mediated endocytosis, but not those of 120 nm. Hatakeyama et al. (2004) concluded that a small size, less than 80 nm is an important factor for the tissue targeting of Tf-SL

* Corresponding author. Tel.: +86 25 83271098.
E-mail addresses: xuemingli@njut.edu.cn (X. Li), pingqn@cpu.edu.cn (Q. Ping).

0378-5173/$ – see front matter © 2009 Elsevier B.V. All rights reserved.
doi:10.1016/j.ijpharm.2009.01.023

based on receptor-mediated endocytosis, especially in the liver and brain. On the other hand, the heart is able to take up both small and large liposomes in a Tf dependent manner. These results suggest that Tf can be the ligand for the active targeting of SL in vivo, and regulation of size confer the tissue selectivity of Tf-SL. Such proteoliposomes may serve as efficient carriers for the transfer of drugs, enzymes, and nucleic acids into cells (Singh, 1999).

Previous studies have demonstrated that doxorubicin-loaded stealth liposomes prolong circulation in the blood (Takeuchi et al., 1999), but create a steric barrier that could cause a reduction in liposomes interaction with the target cells. We hypothesized that Tf-SL might lead to even greater specificity in drug delivery and intracellular retention of cytotoxic drug in the tumor, thereby enhancing therapeutic index. In this study, doxorubicin-loaded stealth liposomes (SL-DOX) were prepared and Tf was conjugated to the surface of SL-DOX to formulate Tf-SL-DOX. During the preparation, the size of liposomes were controlled to less than 100 nm, then studied pharmacokinetics of Free DOX, SL-DOX and Tf-SL-DOX in rats and tissue distribution in tumor-bearing mice.

2. Materials and methods

2.1. Materials

Reagents were obtained from the following sources: 1,2-distearoyl-*sn*-glycero-3-phosphocholine (DSPC), 1,2-distearoyl-*sn*-glycero-3-phosphoethanolamine-N-[carboxy(polyethylene glycol)$_{2000}$] (DSPE–PEG$_{2000}$–COOH) were purchased from Avanti Polar Lipids Inc. N-(3-dimethylaminopropyl)-N′-ethylcarbodiimide hydrochloride (EDC), human holo-transferrin, cholesterol (chol) were from Sigma. Sepharose CL-4B (Pharmacia, USA), and the bicinchoninic acid (BCA) kit for protein determination were from Sigma (Seelze, Germany).

Sulpho-N-hydroxysuccinimide (S-NHS) was from Yanchang bio-science Co. (Shanghai, China). Doxorubicin (DOX) hydrochloride was purchased from Haizheng Pharmaceutical Co. (Zhejiang Province, China). Ammonium sulphate, methanol, and all other chemicals were commercial products of analytical reagent grade.

2.2. Liposome preparation

Liposomes were prepared using a slightly modified protocol according to previously published method (Anabousi et al., 2005; Maruyama et al., 2004). Briefly, the liposome were prepared from cholesterol, DSPC and DSPE–PEG$_{2000}$–COOH at the following molecular ratios: DSPC:chol:DSPE–PEG$_{2000}$–COOH (6:3:0.6, mol%). Briefly, a mixture of phospholipid (PL) and cholesterol in chloroform:methanol (2:1, v/v) was dried to a thin lipid film in a rotary evaporator (BUCHI, R-210, Germany) at 53 °C. Ammonium sulphate (250 mM final concentration) to be encapsulated was then added to result in a final lipid concentration of 10 mg lipid/ml corresponding buffer. After vortexing, the sample was incubated for 10 min at a temperature above the transition temperature of the used lipids (53 °C for DSPC) in a cabinet drier. Unilamellar liposomes were prepared by ultrasonic cell smash instrument (SCIENTZ-IID, China) for 10 min. The liposomes were then extruded five times through each polycarbonate membrane (Nucleopore, USA) of pore sizes 0.4, 0.2, and 0.1 μm consecutively to make smaller size of liposomes.

Doxorubicin was encapsulated into the liposomes using the ammonium sulphate gradient method (Haran et al., 1993; Fritze et al., 2006). Unilamellar liposomes were initially formed in buffer containing ammonium sulphate (250 mM final concentration) as described above. Nonentrapped ammonium sulphate was removed by dialysis. The liposome suspension was then dialyzed in the solution of phosphate-buffered saline (PBS; 129 mM NaCl, 2.5 mM KCl, 7.4 mM $Na_2HPO_4{\cdot}7H_2O$, 1.3 mM KH_2PO_4; pH 7.4) for four times. After dialysis, liposome suspension was placed in another pear-shaped flask in water bath at 60 °C. Subsequently, doxorubicin was added to liposomal dispersion to achieve a drug to PL ratio of 1/9 (w/w). The flask was intermittently shaken in the water bath at 60 °C for 1 h and the doxorubicin stealth liposomes (SL-DOX) were produced.

Conjugation of transferrin to the liposomal surfaces (Grabarek and Gergely, 1990) was achieved by adding 360 μl of both EDC (0.5 M in H_2O) and S-NHS (0.5 M in H_2O) per 10 μmol of lipid, before adjusting to pH 5.2 with citric acid. Excess EDC and S-NHS were removed by dialysis. After adjusting to pH 7.5 with 1 M NaOH, 125 μg Tf/μmol PL were added and gently stirred for 8 h at 4 °C. Unbound protein was removed by passing the liposome suspension through a Sepharose CL-4B gel column.

DOX formulation was administered with sterile saline via intravenous injection. SL-DOX and Tf-SL-DOX were diluted with sterile saline to appropriate concentrations as necessary prior to intravenous injection.

2.3. Methodology of Tf assay

Serum transferrin is a globular glycoprotein (80 kDa) which has often been used as a model protein because of its high aqueous solubility, low affinity for lipids and the ability to bind to specific receptors on cell membranes. Unbound protein was removed by passing the liposome suspension through a Sepharose CL-4B gel column.

The average amount of transferrin conjugated to the liposome was quantified as described by Anabousi et al. (2005). 0.1 ml of liposome suspension was added to 0.4 ml of methanol. The mixture was vortexed and centrifuged (10 s at 1.0×10^4 rpm). Then, 0.2 ml of chloroform was added and the sample was vortexed and centrifuged again (10 s at 1.0×10^4 rpm). For phase separation, 0.3 ml of water was added and the sample was vortexed again and centrifuged for 1 min at 1.0×10^4 rpm. The upper phase was carefully removed and discarded. 0.3 ml of methanol was added to the interphase between chloroform and the precipitated protein. The sample was mixed and centrifuged to pellet the protein (2 min at 1.0×10^4 rpm). The supernatant was removed and the protein pellet was dried under a stream of nitrogen gas. The pellet was then dissolved in 0.1 ml of PBS (pH 7.4) and the concentration was determined with a bicinchonic acid (BCA) protein assay using pure bovine serum albumin as standard. The coupling efficiency was calculated as μg Tf/μmol PL.

2.4. Cell experiments

2.4.1. Cell lines and cell culture

The human hepatoma cell line HepG2, obtained from Cell Institute of Academia Sinica (Shanghai, China), were cultured in RPMI 1640 media supplemented with 10% fetal calf serum (FCS), 100 U/ml penicillin, 100 μg/ml streptomycin at 37 °C in a humidified atmosphere containing 5% CO_2. Cells were plated in 25 ml culture flasks at a density of 10^5 cells/cm^3. The medium was changed every other day.

2.4.2. Flow cytometry analysis

For binding experiments, HepG2 cells were washed twice in PBS and 1×10^6 cells were resuspended in 1 ml of RPMI 1640 medium. The mixture was incubated for 2 h at 37 °C with Tf-SL-DOX, SL-DOX and Free DOX (these DOX preparations have the same concentration of 20 μg/ml), respectively. The cells were then washed three times with ice cold phosphate-buffered saline (PBS, pH 7.4) and analyzed by a FAC Sort flow cytometry (Becton Dickinson, San Jose, CA, USA). Cell-associated DOX was excited with an argon laser (488 nm) and fluorescence was detected at 560 nm. The experiments were

performed in triplicates and 10,000 cells were count in each experiment. The data were analyzed using FAC Station software program.

2.4.3. Intracellular uptake of DOX by confocal microscopy analysis

HepG2 cells (5×10^4 cells/ml) were incubated with Tf-SL-DOX, SL-DOX and Free DOX for 1 h at 37 °C (all the DOX formulations having DOX concentrations of 6.0 μg/ml), washed three times with PBS, fixed in 95% ethanol, and analyzed by a TCS SP2 confocal microscope (Leica, Heidelberg, Germany) at excitation and emission wavelengths of 480 and 540 nm, respectively.

2.4.4. Cytotoxicity assay

The in vitro anticancer effects of drug-loaded liposomes (cytotoxicity) were evaluated using the MTT method. Briefly, the cells were transferred in 100 μl/well of media to 96-well microplates and incubated for 2 days to allow the cells to attach. The cells were exposed to serial concentrations of Free DOX, SL-DOX, Tf-SL-DOX at 37 °C for 8 h in a humidified atmosphere containing 5% CO_2 ($n = 5$) followed by washing with ice cold PBS for three times and replacing with 100 μl of fresh medium. Next, the HepG2 cells were incubated for an additional 40 h. At the end of incubation time, 20 μl of MTT solution (5 mg/ml in PBS (pH 7.4)) was added to each well and the cells were incubated at 37 °C for another 4 h. 200 μl of the supernatant was assayed by measuring the absorbance at dual wavelengths of 570 and 630 nm on an automated plate reader (BIOTEK). HepG2 cells inhibition ratio (as a percentage of control cells) was calculated according to the formula (A570-A630) of treated cells × 100/(A630) of control cells. IC_{50} was defined as the DOX concentration, which was encapsulated in the liposomes or free form that inhibits cell growth by 50% as compared to the control wells without any drug.

2.5. HPLC analysis for DOX

The HPLC system consisted of a Shimadzu pump (LC-10ATvp), a Shimadzu fluorescence detector (RF-10AXL, EX: 480 nm; EM: 550 nm) and a DIKMA Diamonsil C18 column. The mobile phase was 30% (v/v) acetonitrile and 70% 5 mM ammonium acetate, pH 3.5 (Arnold et al., 2004). Flow rate of 1.0 ml/min was used. Measurements were made using the ratio of the peak area of DOX to that of an internal standard (daunomycin).

Standards and quality control stock solutions of DOX (100 μg/ml in methanol) and daunomycin (DNM, 100 μg/ml in methanol) were prepared from individually weighed samples. Calibration samples were prepared fresh by serial dilution of drug standard solutions in mobile phase, plasma, or tissue homogenates. The final DOX concentration ranges in blank rat plasma and in blank tumor-bearing mice tissue were 0.02–4.0 μg/ml and 0.6–12 μg/g, respectively. DNM concentration in blank plasma and blank tissue were 1.0 μg/ml and 3.0 μg/g, respectively.

2.6. Extraction procedures and sample preparation

2.6.1. Plasma extraction

Before the samples were injected into the chromatograph, protein denaturing and precipitation procedures were carried out. Briefly, 750 μl acetonitrile was added to each 200 μl sample to precipitate proteins and extract DOX. 50 μl (4.0 μg/ml) of DNM, the internal standard, was transferred into each sample immediately after the addition of the extraction solvent to plasma, thus achieving a final concentration of 1.0 μg/ml. Samples were mixed, cooled in an ice water bath for 10 min, and centrifuged for 10 min at 14,000 rpm at 4 °C. The deproteinized supernatant was recovered and analyzed immediately.

2.6.2. Tissue extraction

Before homogenizer, 60 μl (5.0 μg/ml) of DNM standard was added to each sample, producing a final concentration of 3.0 μg/g. The tissues were homogenized using a Fluko mechanical homogenizer (F10) in 1.44 ml mobile phase. Samples were cooled in an ice water bath for 10 min, and centrifuged for 10 min at 14,000 rpm at 4 °C. The deproteinized supernatant was recovered and analyzed immediately.

2.7. Animal experiments

2.7.1. Pharmacokinetics of DOX in rats

The animals were randomly divided into experimental groups (eight rats per group) for treatment with formulations of DOX, SL-DOX, and Tf-SL-DOX. Formulations at doses of DOX (5 mg/kg) were administered via the tail vein (administration rate 0.4 ml/min). After injection, blood was serially sampled from retro-orbital sinus at 5, 10, 15, 30, and 45 min, 1, 2, 4, 8, 12, 24, 36, 48, 72, and 96 h. Blood samples (600 ml) were collected in heparinized tubes, and then centrifuged at 3000 rpm for 10 min at 4 °C to separate the plasma and stored at −20 °C until assayed for DOX.

2.7.2. Tissue distribution of DOX in tumor-bearing mice

HepG2 cells (1×10^6 cells/0.2 ml) were injected subcutaneously into in the right flank of the male ICR mice (China Pharmaceutical University, Nanjing, China) and tumors were allowed to develop. At day 10 after tumor implantation, animals bearing tumors of about 400 mm^3 were used in the study.

The mice in groups of five to six animals were given DOX, SL-DOX and Tf-SL-DOX at a single injection of 5 mg DOX/kg via tail vein. At indicated times after injection, the mice were then sacrificed by cervical dislocation, and the heart, liver, spleen, lung, kidney and tumor were immediately excised. These tissues were then lightly blotted to remove any excess blood, weighed and stored at −20 °C until assayed for DOX.

2.7.3. Antitumor activity in vivo

Tf-SL-DOX, SL-DOX and Free DOX were injected into the tumor-bearing mice (described in 2.7.2, 10 per group) via the tail vein at 1.5 or 3 mg DOX/kg according to the mean weight of each treatment group. The size of the tumor and body weight of each mouse was monitored thereafter. The antitumor effect of DOX preparations was evaluated on the basis of the changes in tumor volume and weight at selected time intervals (1 day) after administration. At day 9, the mice were sacrificed and the tumor was harvested. For determining the tumor volume, two bisecting diameters of each tumor were measured with slide calipers to determine the tumor volume; and calculation was performed using the formula $0.5(ab^2)$, where a is the largest, and b, the smallest diameter (mm) of the tumor, respectively. All animal experiments were performed in accordance with China Pharmaceutical University institutional guidelines for the care and use of animals.

2.8. Data analysis

The plasma concentration data were fitted using 3P97 pharmacokinetic software, to calculate the area under the curve (AUC), terminal elimination half-life ($T_{1/2\beta}$), plasma clearance (CL) and elimination rate constant. Appropriate models fitting the plasma concentrations data were evaluated by criteria according to the goodness of fit for each model. These included the objective function, visual assessment of distribution of residuals, and Akaike's Information Criterion (AIC). Data were presented as mean ± S.D. Statistical analyses were performed using one-way ANOVA followed by post hoc Tukey HSD test, and statistical significance was set at $P < 0.05$.

3. Results

3.1. Physical properties of the liposomes

The physical properties of the liposomes before and after coupling of Tf are given in Tables 1 and 2. The size of the liposomes before conjugation of Tf was in the range of 62 nm. After the addition of Tf, the average size increased between 5 and 10 nm for all samples under investigation. The PI did not show any significant alteration, indicating that the stability of the liposomes has not been negatively affected. Values for the *z*-potential were between −20 and −40 mV for the liposomes.

Entrapment efficiency of liposomes, concentration of doxorubicin, the amount of Tf (assessed by BCA assay) in correlation to the amount of total phospholipid (assessed according to Derycke and de Witte, 2002) are given in Table 2.

3.2. Extraction efficiency

A simple and rapid extraction procedure was developed which provides a consistent matrix composition between samples and minimizes the potential for concentration dependent variation in protein binding. Total extraction time was approximately 20 min for batches of 15–20 samples. The efficiency of DOX extraction was determined by comparison of DOX standards extracted from plasma and tissue homogenates to DOX standards prepared in mobile phase. For the plasma of interest, the efficiency of DOX extraction was 71–87% over the concentration range of 0.02–4.0 μg/ml DOX, which is relevant to in vivo samples. For the tissues of interest, the efficiency of DOX extraction was 16–93% over the concentration range of 0.6–12.0 μg/g DOX, which is relevant to in vivo samples.

3.3. Cellular uptake of DOX by flow cytometry

Flow cytometry was used to quantify the total DOX uptake by HepG2 cells for different DOX formulations. As shown in Fig. 1, the cellular DOX level for Tf-SL-DOX in HepG2 cells was higher than that of SL-DOX.

3.4. Confocal microscopy of interactions of DOX formulations with the cells

The extent of cell association of the different DOX formulations with HepG2 cells was further evaluated by confocal microscopy (Fig. 2), after exposure for 1 h, Tf-SL-DOX were efficiently internalized by the cells and the level of cellular uptake was significantly higher than that of non-targeted control liposomes based on Fig. 2.

Flow cytometry studies and confocal microscopy analysis demonstrated that association of targeted liposomes (Tf-SL-DOX) to HepG2 cells occurs at a significantly larger extent than non-targeted formulations (SL-DOX).

3.5. Cytotoxicity activity

The cytotoxicity of Tf-SL-DOX, SL-DOX and Free DOX to HepG2 cells was compared. DOX concentrations leading to 50% cell-killing (IC_{50}) were determined from concentration-dependent cell viability curves. The IC_{50} of Tf-SL-DOX, SL-DOX and Free DOX against the HepG2 cells were 5.22,20.4, and 166.2 μmol/L, respectively. Fig. 3 shows the inhibition ratio of DOX of different concentrations for different preparations of DOX. The IC_{50} of targeted Tf-SL-DOX was significantly lower than that of SL-DOX. These results indicate that Tf was effective in promoting the internalization of liposomes encapsulating DOX to the target tumor cells. DOX-loaded Tf-SL provided the most efficient killing of cancer cells compared to DOX in plain SL.

Table 1
Size, polydispersity index (PI) and ζ-potential of liposomes before and after coupling of transferrin at pH 7.4. Data are shown as means and standard deviation ($n = 3$).

Physical properties	Before addition of transferrin	After addition of transferrin
Size (nm)	62 ± 17	70 ± 19
PI	0.231 ± 0.02	0.253 ± 0.03
ζ-potential (mV)	−19.65 ± 1.15	−30.33 ± 2.08

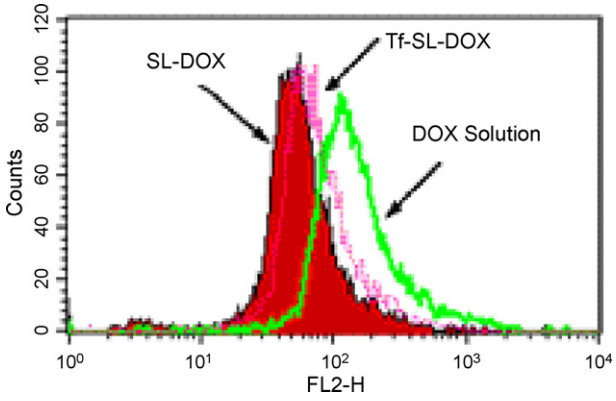

Fig. 1. Flow cytometric measurement of doxorubicin uptake by HepG2 cells after incubated with SL-DOX, Tf-SL-DOX and Free DOX. HepG2 cells were washed twice in PBS and 1×10^6 cells were resuspended in 1 ml of RPMI 1640 medium. The mixture was incubated for 2 h at 37 °C with Tf-SL-DOX, SL-DOX and Free DOX, respectively. The cells were then washed with ice cold phosphate-buffered saline (PBS, pH 7.4) and analyzed by a FAC Sort flow cytometry.

3.6. Plasma pharmacokinetics

Fig. 4 illustrates the DOX concentration in plasma–time profiles of Free DOX, SL-DOX and Tf-SL-DOX. DOX concentration in plasma–time data with Free DOX, SL-DOX and Tf-SL-DOX, were all best fitted with a three-compartment model, characterized by an initial rapid phase of drug concentration decrease, and a slower terminal elimination phase. The pharmacokinetic parameters are shown in Table 3. The pharmacokinetics parameters of Free DOX were characterized with an $AUC_{0-12\,h}$ of 537.8 ng h/ml, a terminal half-life ($T_{1/2\beta}$) of 5.476 h.

When formulations containing liposomal DOX were administered, the plasma concentration–time profiles were entirely different from DOX. It showed that liposomal DOX significantly altered some pharmacokinetic parameters of DOX (Table 3). Liposomal DOX increased significantly the $AUC_{0-96\,h}$ and reduced CLp

Table 2
Entrapment efficiency, concentration of doxorubicin, transferrin amount, phospholipids amount and coupling efficiency. Data are shown as means and standard deviation ($n = 3$).

Entrapment efficiency	Concentration of doxorubicin (mg/ml)	Tf amount (μg/ml)	PL amount (μmol/ml)	Coupling efficiency (μg Tf/μmol PL)
96.4%	0.54	511.4	5.20	98.3
95.5%	0.51	482.3	4.99	96.7
96.8%	0.53	500.4	4.71	106.2

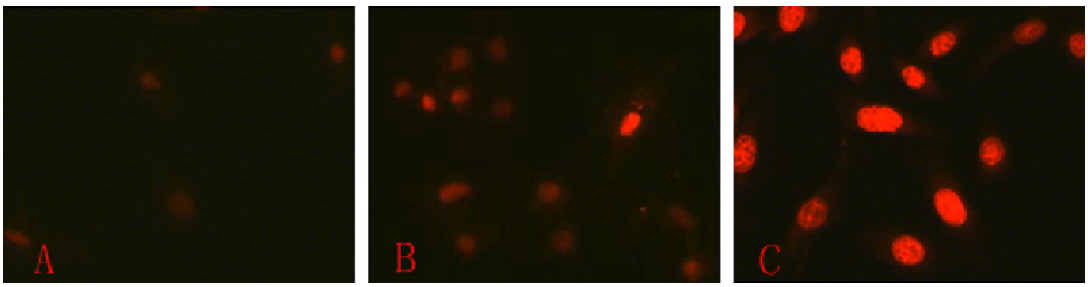

Fig. 2. Confocal laser scanning microscopy of HepG2 cells (5×10^4 cells/ml) after incubation with SL-DOX (A), Tf-SL-DOX (B) and Free DOX (C) for 1 h at 37 °C, washed three times with PBS, fixed in 95% ethanol, and analyzed by a TCS SP2 confocal microscope. All these DOX formulations having DOX concentrations of 6.0 μg/ml.

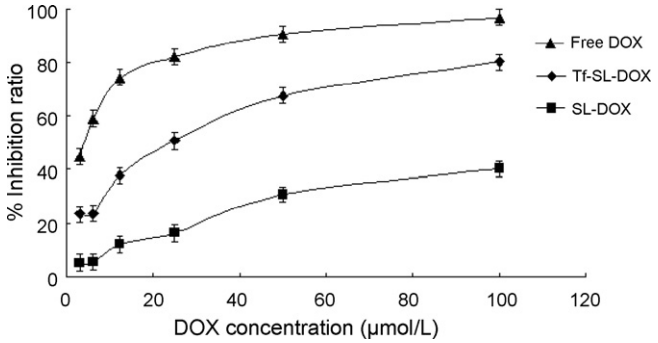

Fig. 3. 48 h cytotoxicity assay of SL-DOX, Tf-SL-DOX and Free DOX to HepG2 cells. Data are represented as percentage of control. Each assay was done in triplicate (mean ± S.D.). The cells were exposed to serial concentrations of Free DOX, SL-DOX, Tf-SL-DOX at 37 °C for 8 h. The cytotoxicity was evaluated using the MTT method. HepG2 cells inhibition ratio (as a percentage of control cells) was calculated according to the formula (A570–A630) of treated cells × 100/(A630) of control cells.

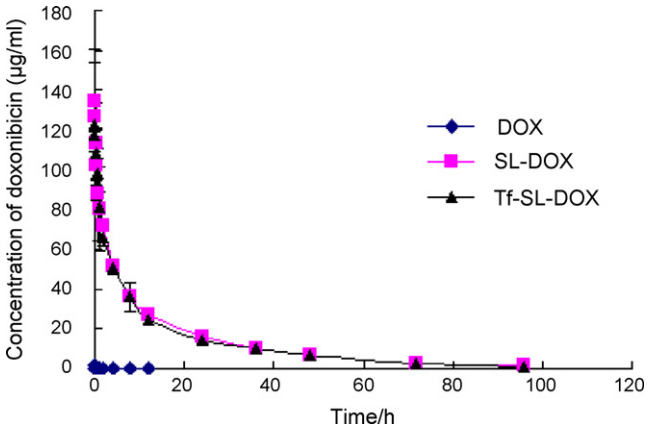

Fig. 4. Plasma DOX concentration–time profiles of Free DOX (□), SL-DOX (■) and Tf-SL-DOX (▲). DOX in solution or within SL- or Tf-SL-liposomes (DOX: 5 mg/kg) was injected via tail veins of rats. At various times thereafter, blood samples were collected using glass capillaries from veins of fundus oculi. Plasma DOX levels were measured by HPLC. Data are shown as means and standard deviation (n = 5–6).

of DOX. Compared with Free DOX treatment, an $AUC_{0-96\,h}$ of 1.22 mg h/ml obtained from the Tf-SL-DOX treatment represented a very significant 2400-fold increase in AUC, confirming slower DOX removal from the plasma compartment of DOX-encapsulated liposome. An elimination $T_{1/2\beta}$ of 22.4 h was 4-fold higher and CLp was 2500-fold slower when compared to Free DOX. But V_C for Free DOX was 200-fold more than that of Tf-SL-DOX. However, with SL-DOX, the pharmacokinetic parameters were similar to that with Tf-SL-DOX (Table 3), suggesting that liposomes modified with transferrin had no effects on the pharmacokinetics of liposomal DOX (SL-DOX).

3.7. Tissue distribution

The DOX levels and distribution characteristics after i.v. injection of Free DOX, SL-DOX or Tf-SL-DOX at the dose of 5 mg/kg were shown in Fig. 5. At 1 h after administration of the preparations of Free DOX, DOX concentration was found in kidney > spleen > liver > lung > heart > tumor. Distribution of DOX at 1 h point to the heart and kidney was significantly reduced by intra-

Table 3
Summary of pharmacokinetic parameters for Free DOX, SL-DOX and Tf-SL-DOX.

Parameters	Unit	DOX	SL-DOX	Tf-SL-DOX
P	μg/ml	5.956 ± 1.621	63.728 ± 12.189	52.297 ± 13.450
pi	h^{-1}	15.451 ± 3.060	2.542 ± 1.313	0.963 ± 0.480
A	μg/ml	0.120 ± 0.151	49.105 ± 6.148	45.654 ± 11.470
α	h^{-1}	2.791 ± 3.323	0.201 ± 0.043	0.152 ± 0.119
B	μg/ml	0.012 ± 0.000	33.520 ± 6.246	24.328 ± 9.636
β	h^{-1}	0.133 ± 0.041	0.034 ± 0.002	0.031 ± 0.003
V_C	L/kg	4.000 ± 1.000	0.150 ± 0.025	0.205 ± 0.015
$T_{1/2}$(pi)	h	0.046 ± 0.009	0.339 ± 0.202	0.843 ± 0.379
$T_{1/2}(\alpha)$	h	0.853 ± 1.015	3.551 ± 0.709	6.398 ± 3.627
$T_{1/2}(\beta)$	h	5.476 ± 1.690	20.584 ± 0.905	22.238 ± 2.059
K12	h^{-1}	0.967 ± 0.308	0.923 ± 0.537	0.273 ± 0.063
K21	h^{-1}	3.086 ± 3.704	1.523 ± 0.790	0.627 ± 0.437
K13	h^{-1}	2.796 ± 2.040	0.117 ± 0.034	0.072 ± 0.080
K31	h^{-1}	0.162 ± 0.029	0.099 ± 0.018	0.073 ± 0.044
K10	h^{-1}	11.363 ± 0.319	0.115 ± 0.004	0.100 ± 0.004
AUC	(μg/ml) h	0.538 ± 0.145	1276.458 ± 195.444	1221.262 ± 80.795
CL(s)	L/(kg h)	50.000 ± 1.500	0.020 ± 0.005	0.020 ± 0.000
MRT	h	2.431 ± 0.050	23.464 ± 1.128	22.585 ± 2.594

The plasma concentration data were fitted using 3P97 pharmacokinetic software. Appropriate models fitting the plasma concentrations data were evaluated by criteria according to the goodness of fit for each model. Data are shown as means and standard deviation (n = 5–6).

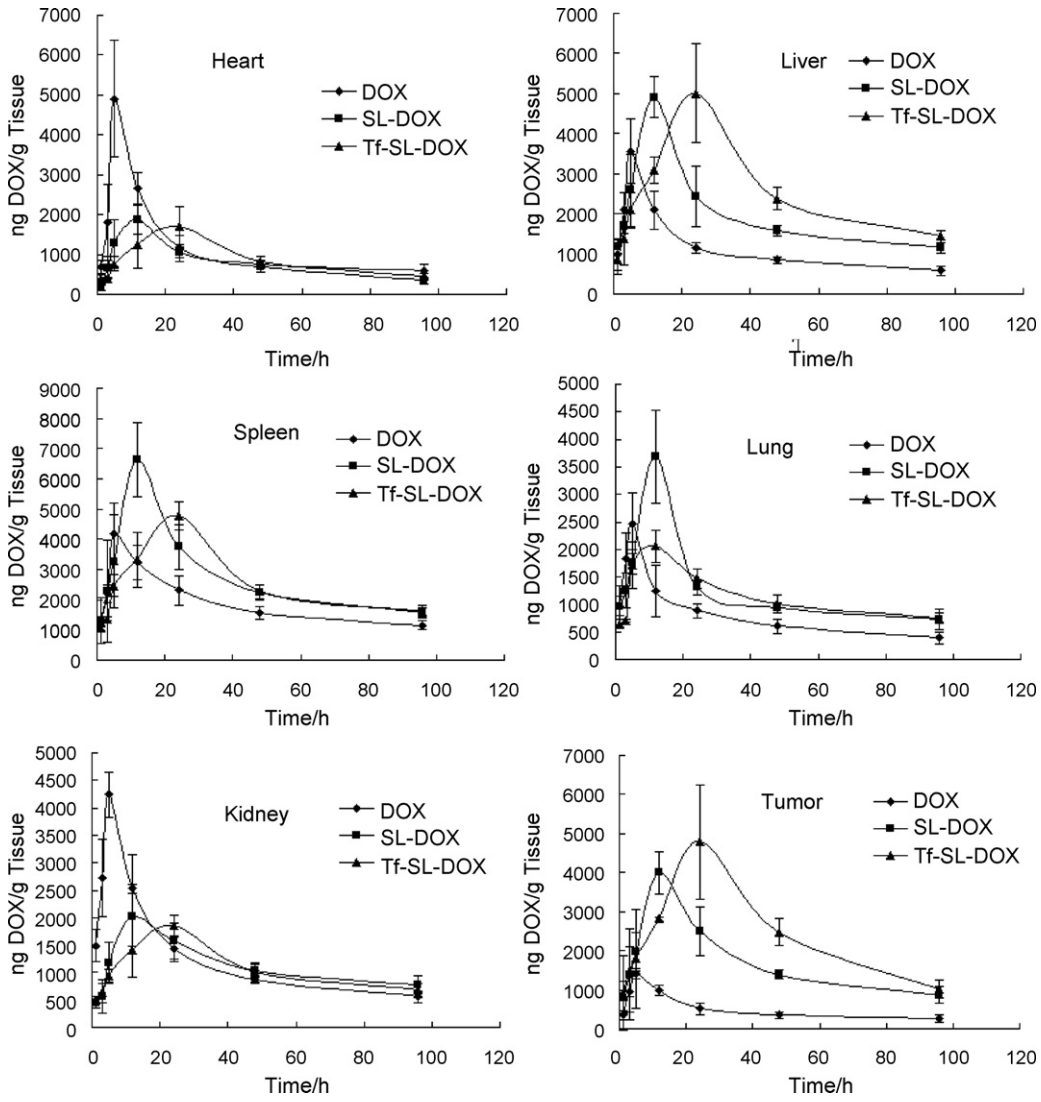

Fig. 5. Tissues distribution of mice after i.v. injection of Free DOX (□), SL-DOX (■) and Tf-SL-DOX (▲). DOX in solution or within SL- or Tf-SL-liposomes (DOX: 5 mg/kg) was injected via tail veins of tumor-bearing mice. At various times thereafter, the mice were then sacrificed by cervical dislocation, and the heart, liver, spleen, lung, kidney and tumor were immediately excised. DOX levels were measured by HPLC. Data are shown as means and standard deviation ($n = 5–6$).

venously administered SL-DOX or Tf-SL-DOX, but significantly increased in tumor.

It was showed that at 5 h after administration of Free DOX, the highest DOX concentration was found in all tissues. With SL-DOX and Tf-SL-DOX treatment, the highest DOX concentration was found at 12 and 24 h in all tissues, respectively. At 1, 3, 5 and some including 12 h, the distribution of DOX to heart, liver, lung, kidney for liposomal DOX (SL-DOX, Tf-SL-DOX) were reduced when compared to the Free DOX. At 12, 24, 48 and 96 h, DOX concentration of SL-DOX and Tf-SL-DOX were obviously higher than Free DOX in liver, spleen, lung, tumor, some in heart and kidney. It is interesting to note that significant increase of DOX contents in tumor tissue was observed for the SL-DOX and Tf-SL-DOX compared to that of Free DOX all the times.

The area under the DOX concentration–time curves (AUC) calculated for 1–96 h in these tissues is listed in Table 4. The calculated AUC of SL-DOX and Tf-SL-DOX in tumor were 3.6- and 5.2-fold higher than that of Free DOX, respectively. In addition, SL-DOX and Tf-SL-DOX also produced significantly increased AUC in liver ($P < 0.01$), spleen ($P < 0.01$), lung ($P < 0.01$), tumor ($P < 0.01$), significantly reduced AUC in heart ($P < 0.01$). Similar AUC was observed in heart, spleen, lung and kidney for SL-DOX and Tf-SL-DOX formulations. It is noteworthy that the mice treated with Tf-SL-DOX demonstrated remarkably higher AUC ($P < 0.01$) than SL-DOX in tumor. As anticipated, Tf-SL-DOX and SL-DOX displayed a much greater systemic circulation time than Free DOX, which showed rapid clearance kinetics.

Table 4
AUC values in various tissues of mice after i.v. injection of Free DOX, SL-DOX and Tf-SL-DOX.

Formulation	Tissue[a] AUC (h μg/g)					
	Heart	Liver	Spleen	Lung	Kidney	Tumor
Free DOX	114.4	105.8	180.9	74.5	120.0	46.1
SL-DOX	77.6**	190.9*	269.3*	121.1*	110.4	166.1*
Tf-SL-DOX	87.2**	252.9*	253.0*	110.2*	105.1	238.7*,***

DOX in solution or within SL- or Tf-SL-liposomes (DOX: 5 mg/kg) was injected via tail veins of tumor-bearing mice. At various times thereafter, the mice were then sacrificed by cervical dislocation, and the heart, liver, spleen, lung, kidney and tumor were immediately excised. DOX levels were measured by HPLC.

[a] AUC values are calculated for 1–96 h.

* $P < 0.01$, vs. Free DOX.

** $P < 0.01$, vs. Free DOX.

*** $P < 0.01$, vs. SL-DOX.

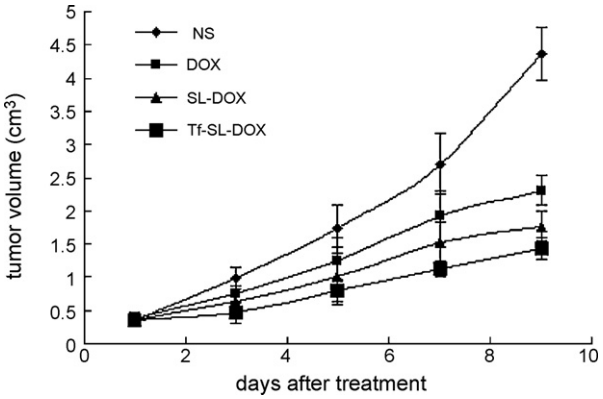

Fig. 6. Suppression of tumor growth by Free DOX, SL-DOX or Tf-SL-DOX. ICR mice with Heps tumor were given a single i.v. injection of Free DOX, SL-DOX or Tf-SL-DOX at a dose of 3 mg/kg at 2 weeks post-inoculation, respectively. Tumor size was measured for each animal daily. Results are given as means ± S.D. (n = 10).

In addition, as illustrated in Fig. 5, Tf-SL-DOX show delayed peak time in most of tissues compared to SL-DOX, we supposed that it may be attributed to the delayed release effect caused by Tf on the surface of the Tf-SL-DOX. It will be confirmed in our later study.

3.8. Antitumor efficiency

Mice bearing Heps tumors were injected with DOX in solution or encapsulated within various liposomes at a dose of 1.5 or 3 mg/kg. Mice were given saline as a control. Tumor growth inhibition curves in terms of mean tumor size (cm^3) were presented in Fig. 6. As shown in Fig. 6, at a dose of 3 mg/kg, all the DOX formulations were effective in preventing tumor growth compared to saline. Treatment with Tf-SL-DOX displayed stronger tumor inhibition than treatment with SL-DOX.

The therapeutic effects examined by measuring the suppression of tumor growth in weight have also confirmed the highest efficiency of drug loaded Tf-SL (Fig. 7), the average weight of excised tumors in the group treated with DOX incorporated in Tf-SL approximated 0.33 g compared to approximate 1.38 and 1.17 g weight in groups treated with Free drug or drug in plain PEG-SL, respectively (the weight of untreated tumors approximated 2.00 g,

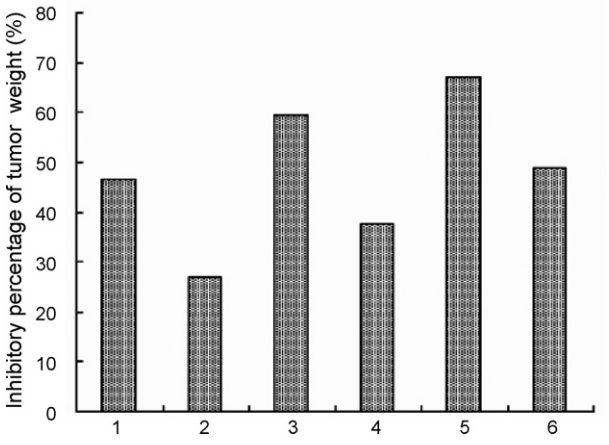

Fig. 7. Tumor growth inhibition ratio by Free DOX, SL-DOX or Tf-SL-DOX. ICR mice with Heps tumor were given a single i.v. injection of DOX (high dose: 3 mg/kg, low dose: 1.5 mg/kg) at day 9 post-tumor implantation, tumor growth inhibition ratio was represented as the ratio for the tumor volume on day 10 (before DOX treatment) after tumor cell inoculation to that on day 9 after DOX treatment (n = 10), ((1) Free DOX group of high dose; (2) Free DOX group of low dose; (3) SL-DOX group of high dose; (4) SL-DOX group of low dose; (5) Tf-SL-DOX group of high dose; (6) Tf-SL-DOX group of low dose).

$P < 0.05$ in all cases). Tumor growth was obviously suppressed by DOX encapsulated within Tf-SL-DOX compared to DOX in solution and encapsulated within SL-DOX. As anticipated, Tf-SL-DOX showed strong tumor growth suppression than SL-DOX and Free DOX.

4. Discussion

DOX is one of the most widely used broad spectrum anticancer agents and it has been in clinical use against a wide range of human cancers for decades. Nevertheless, a number of issues critical to the therapeutic success and safety of the drug, such as cardiotoxicity, drug resistance, and specificity remain to be improved. In addition, DOX exerts antitumor activity after intercalating with the double-stranded helix DNA in nuclei (Gewirtz, 1999). Thus, intracellular delivery of DOX into tumor cells will be essential to its antitumor activity. It was well established that Tf-SL was an effective potential target carrier for specific drug delivery into tumor cells. Tf-SL showed a prolonged residence time in the circulation and low RES uptake in tumor-bearing mice, resulting in enhanced extravasation of the liposomes into the solid tumor tissue. This phenomenon has been characterized and termed the tumor-selective enhanced permeability and retention effect of macromolecules and lipidic particles including liposomes. The Tf-SL-DOX that we prepared here appear to satisfy these requirements and are very useful for cancer chemotherapy.

It has been determined that the size of liposomes is an important factor for the tissue targeting of Tf-SL based on receptor-mediated endocytosis. As expected, we prepared small liposomes with a size of 60–80 nm. Tf-SL-DOX were achieved by the use of functionalized PEG derivatives to couple transferrin directly to the distal terminal of PEG chains incorporated in liposomes.

The stability test of liposomes (stored in refrigerator at 4 °C for 60 days) demonstrated that the leakage ratio of drug from Tf-SL-DOX was only 0.39%. Gradients of ammonium sulphate in liposomes were used to obtain active loading of amphipathic weak bases into the aqueous compartment of liposomes. This approach was applied to encapsulate doxorubicin inside the liposomes at very high efficiency (>90%). Most of the intraliposomal doxorubicin was present in an aggregated state. The stability of the ammonium ion gradient is related to the low permeability of its counterion, the sulphate, which also stabilizes doxorubicin accumulation for prolonged storage periods (>6 months) due to the aggregation and gelation of doxorubicin sulphate salt.

Tf-SL-DOX and SL-DOX can passively accumulate into the tumor tissues by the effect of EPR. Park et al. (2000) demonstrated that following intravenous administration, the DOX-entrapped liposomes predominantly accumulated in the interstitial fluid of extracellular and perivascular space of the tumor. Liposomes diffusion into the interstitial fluid of the tumor was heavily dependent on the liposomal AUC in the blood stream. However, as mentioned above, SL-DOX cannot directly enter the tumor cells, so the extracellular release in the interstitial fluid becomes the determinant step for the intracellular delivery of DOX by tumor cells. The released DOX from SL-DOX will follow the same pathway as for free drugs in terms of cellular drug uptake, metabolism and efflux. In vivo environment, the accumulated SL-DOX or the released DOX in the interstitial fluid, if not be arrested timely by the tumor cells, will redistribute away from the tumor cells. As a result, DOX that actually delivered into the tumor cells by SL-DOX would be not different from that by Free DOX, leading to a similar therapeutic efficiency for them. In contrast, Tf-SL-DOX can efficiently deliver the drugs into the tumor cells by the receptor-mediated endocytosis and lead to a high concentration of DOX in the tumor cells. Similar observations have been found in other studies where various ligands are

employed (Gibizon et al., 2004; Xiong et al., 2005; Cheng, 1996), so whether it means a similar targeting mechanism was involved needs to be further investigated.

We have demonstrated that liposomal DOX did altered some pharmacokinetic parameters and tissue distribution of DOX. Liposomal DOX increased significantly the AUC_{0-t} and reduced CLp of DOX. An elimination $T_{1/2\beta}$ of 22.4 h was 4-fold higher when compared to Free DOX. However, liposomes modified by transferrin (Tf-SL-DOX) had no effects on the pharmacokinetics of SL-DOX (Table 3), suggesting that liposomes modified with transferrin had no effects on the pharmacokinetics of liposomal DOX (SL-DOX). We estimated the main reason for this phenomena is that the difference in pharmaceutics characters such as particle size and encapsulation efficiency between Tf-SL-DOX and SL-DOX is negligible.

Administration of Tf-SL-DOX to tumor-bearing mice could be used to deliver DOX effectively to the targeted site, significantly increasing DOX content in tumor and decreasing DOX content in heart and kidney. It resulted in more favorable pharmacodynamics in terms of reduced acute cardiotoxicity. This would improve the therapeutic index of DOX, and is a proof of principle in support of administering liposomally co-encapsulated drug.

The adverse effect is a major concern for the Tf-SL as a potential drug delivery system, because transferrin receptor that recognize transferrin could also be found in some normal cells. Thus, the intracellular DOX uptake by normal cells and the cytotoxicity on these cells might be enhanced by Tf-SL. However, we found that Tf-SL-DOX did not increase DOX accumulation in spleen, lungs, more importantly, in heart, which is most sensitive to DOX toxicity. Further, the over-expression of transferrin receptor on tumor endothelium or tumor cells could strength the targeting ability of the Tf-modified SL. Therefore, regarding cardiotoxicity, Tf-SL-DOX should be equivalent to SL-DOX. It is noteworthy that the highest DOX concentration was found at 5, 12 and 24 h in all tissues with DOX, SL-DOX and Tf-SL-DOX treatment, respectively. As anticipated, Tf-SL-DOX, SL-DOX displayed a much greater systemic circulation time than Free DOX, which showed rapid clearance kinetics.

There were some reports related to Tf-SL-DOX, Anabousi assessed the uptake levels and cytotoxicity of Tf-conjugated doxorubicin-loaded liposomes in vitro. The results suggested that Tf-conjugated doxorubicin-loaded liposomes showed enhanced cytotoxicity towards cancerous human pulmonary epithelial cell lines in comparison to noncancerous human alveolar ATI/ATII cells in primary culture. The studies concluded that Tf-modified liposomes might be promising candidates for an aerosol therapy of lung cancer (Anabousi et al., 2006).

In our study, we studied the intracellular uptake, pharmacokinetics and biodistribution of Tf-SL-DOX, and summarized that Tf-modified SL was able to enhance the intracellular uptake of the entrapped DOX by HepG2 cells and improve the therapeutic efficacy of liver cancer.

5. Conclusion

Based on the results in this study, it is suggested that Tf-modified SL could be employed to enhance the intracellular delivery of anticancer agents such as cytotoxic drugs, antisense nucleic acids, ribozymes or imaging agents, etc.

Acknowledgement

The authors wish to thank the Natural Science Foundation of Jiangsu province (BK2006177) for the financial support of this work.

References

Anabousi, S., Laue, M., Lehr, C.M., Bakowsky, U., Ehrhardt, C., 2005. Assessing transferrin modification of liposomes by atomic force microscopy and transmission electron microscopy. Eur. J. Pharm. Biopharm. 60, 295–303.

Anabousi, S., Bakowsky, U., Schneider, M., Huwer, H., Lehr, C.M., Ehrhardt, C., 2006. In vitro assessment of transferrin-conjugated liposomes as drug delivery systems for inhalation therapy of lung cancer. Eur. J. Pharm. Sci. 29, 367–374.

Arnold, R.D., Slack, J.E., Straubinger, R.M., 2004. Quantification of doxorubicin and metabolites in rat plasma and small volume tissue samples by liquid chromatography/electrospray tandem mass spectroscopy. J. Chromatogr. B 808, 141–152.

Ceh, B., Winterhalter, M., Frederik, P.M., Vallner, J.J., Lasic, D.D., 1997. Stealth liposomes: from theory to product. Adv. Drug Deliv. Rev. 24, 165–177.

Cheng, P.W., 1996. Receptor-ligand facilated gene transfer: enhancement of liposome mediated gene transfer and expression by transferrin. Hum. Gene Ther. 7, 275–282.

Derycke, A.S., de Witte, P.A., 2002. Transferrin-mediated targeting of hypericin embedded in sterically stabilized PEG-liposomes. Int. J. Oncol. 20, 181–187.

Fritze, A., Hens, F., Kimpfler, A., Schubert, R., Süss, R.P., 2006. Remote loading of doxorubicin into liposomes driven by a transmembrane phosphate gradient. Biochim. Biophys. Acta 1758, 1633–1640.

Gewirtz, D.A., 1999. A critical evaluation of the mechanisms of action proposed for the antitumor effects of the anthracycline antibiotics adriamycin and daunorubicin. Biochem. Pharmacol. 57, 727–741.

Gibizon, A., Hilary, S., Shmeeda, H., Horowitz, A.T., Zalipsky, S., 2004. Tumor cell targeting of liposome-entrapped drugs with phospholipid-anchored folic acid-PEG conjugates. Adv. Drug Deliv. Rev. 56, 1177–1192.

Grabarek, Z., Gergely, J., 1990. Zero-length crosslinking procedure with the use of active esters. Anal. Biochem. 185, 131–135.

Haran, G., Cohen, R., Bar, L.K., Barenholz, Y., 1993. Transmembrane ammonium sulfate gradients in liposomes produce efficient and stable entrapment of amphipathic weak bases. Biochim. Biophys. Acta 1151, 201–215.

Harrington, K.J., Mohammadtaghi, S., Uster, P.S., Glass, D., Peters, A.M., Vile, R.G., Stewart, J.S., 2001. Effective targeting of solid tumors in patients with locally advanced cancers by radiolabeled pegylated liposomes. Clin. Cancer Res. 7, 243–254.

Harvie, P., Wong, F.M., Bally, M.B., 2000. Use of poly(ethylene glycol)–lipid conjugates to regulate the surface attributes and transfection activity of lipid–DNA particles. J. Pharm. Sci. 89, 652–663.

Hatakeyama, H., Akita, H., Maruyama, K., Suhara, T., Harashima, H., 2004. Factors governing the in vivo tissue uptake of transferring-coupled polyethylene glycol liposomes in vivo. Int. J. Pharm. 281, 25–33.

Ishida, O., Maruyama, K., Tanahashi, H., Iwatsuru, M., Sasaki, K., Eriguchi, M., Yanagie, H., 2001. Liposomes bearing polyethyleneglycol-coupled transferrin with intracellular targeting property to the solid tumors in vivo. Pharm. Res. 18, 1042–1048.

Joo, S.Y., Kim, J.S., 2002. Enhancement of gene transfer to cervical cancer cells using transferrin-conjugated liposome. Drug Dev. Ind. Pharm. 28, 1023–1031.

Maeda, H., Wu, J., Sawa, T., Matsumura, Y., Hori, K., 2000. Tumor vascular permeability and the EPR effect in macromolecular therapeutics: a review. J. Control. Release 65, 271–284.

Maruyama, K., Ishida, O., Kasaoka, S., Takizawa, T., Utoguchi, N., Shinohara, A., Chiba, M., Kobayashi, H., Eriguchi, M., Yanagie, H., 2004. Intracellular targeting of sodium mercaptoundecahydrododecaborate (BSH) to solid tumors by transferrin-PEG liposomes, for boron neutron-capture therapy (BNCT). J. Control. Release 98, 195–207.

Park, J.W., Kirpotin, D.B., Hong, K., Shalaby, R., Shao, Y., Nielsen, U., Marks, J., Papahadjopoulos, D., 2000. Anti-HER2 immunoliposomes: enhanced efficacy via intracellular delivery. Proc. Am. Assoc. Cancer Res. 41, 524.

Qian, Z.M., Li, H.Y., Sun, H.Z., Ho, K., 2002. Targeted drug delivery via the transferrin receptor mediated endocytosis pathway. Pharmacol. Rev. 54, 561–587.

Singh, M., 1999. Transferrin as a targeting ligand for liposomes and anticancer drugs. Curr. Pharm. Design 5, 443–451.

Singh, M., Atwal, H., Micetich, R., 1998. Transferrin directed delivery of adriamycin to human cells. Anticancer Res. 18, 1423.

Takeuchi, H., Kojima, H., Toyoda, T., Yamamoto, H., Hino, T., Kawashima, Y., 1999. Prolonged circulation time of doxorubicin-loaded liposomes coated with a modified polyvinyl alcohol after intravenous injection in rats. Eur. J. Pharm. Biopharm. 48, 123–129.

Vertut-Doi, A., Ishiwata, H., Miyajima, K., 1996. Binding and uptake of liposomes containing a poly (ethylene glycol) derivative of cholesterol (stealth liposomes) by the macrophage cell line J774: influence of PEG content and its molecular weight. Biochim. Biophys. Acta 1278, 19–28.

Xiong, X.B., Huang, Y., Lu, W.L., Zhang, X., Zhang, H., Nagai, T., Zhang, Q., 2005. Enhanced intracellular delivery and improved antitumor efficacy of doxorubicin by sterically stabilized liposomes modified with a synthetic RGD mimetic. J. Control. Release 107, 262–275.